RESULTS OF THE APT RF POWER COUPLER DEVELOPMENT FOR SUPERCONDUCTING LINACS*

E. N. Schmierer†, W. B. Haynes, F. L. Krawczyk, D. C. Gautier, J. G. Gioia, M. A. Madrid, R. E. Lujan, K. C. D. Chan, D. Schrage, B. G. Smith, J. Waynert; LANL, Los Alamos, NM 87545, USA
B. Rusnak; Lawrence Livermore National Laboratory, Livermore, CA 94550, USA

Abstract

For the new baseline APT (Accelerator Production of Tritium) linac design, the power couplers are required to transmit 420 kW of CW RF power to the superconducting cavities at 700 MHz. These couplers consist of an airside waveguide-to-coax transition, an air/vacuum break made by two planar, coaxial windows, and a vacuum-side coaxial antenna section. The coaxial antenna allows adjustability of the RF matching to the superconducting cavities. Design, fabrication, and testing of the power coupler/window occurred over the last four years, and room temperature testing of the prototype design is complete. Coupler/window assemblies have transmitted power to 1 MW, CW and have handled full reflected 850 kW, CW over a limited standing-wave phase range. Couplers were tested with a portion of the outer conductor cooled by liquid nitrogen to study the effects of condensed gases. No hard multipacting barriers were encountered during any of this room temperature testing. Final results, conclusions, and lessons learned about the coupler design, fabrication, and testing will be discussed.

1 OVERVIEW AND REQUIREMENTS

The power coupler was one of the challenges for the Accelerator Production of Tritium (APT) linac, which has a high-energy superconducting (SC) section spanning 210–1030 MeV [1]. Due to the 100 mA proton current, a large amount of continuous wave (CW) radio frequency (RF) power must be transmitted into the SC cavities through the input power coupler. In 1997, the coupler requirement of 210 kW, CW (at 700 MHz) was chosen for the APT couplers as a reasonable extrapolation of the technology at that time. Later, due to testing results, this was increased to 420 kW, CW requiring only one input power coupler per cavity. Multipacting and window failure concerns governed the design features of the coupler/window assembly. Figure 1 shows the APT coupler layout and its relationship to the cavity.

2 ASSEMBLY DESIGN

2.1 Coupler & RF Window Assembly Design

The entire assembly consists of two main components, the RF window assembly and the power coupler. The RF window assembly consists of a WR 1500 waveguide-to-coaxial conductor (50 Ohm, ϕ152-mm) tee-bar transition containing the dual, ceramic windows (Fig. 2). The power coupler consists of the outer conductor (OC), inner conductor (IC), and the thermal intercept. The power coupler interfaces the RF window assembly with a vacuum flange at the respective outer conductors and at the tee bellows for the inner conductors. The OC contains a 4-way, ϕ152-mm coaxial tee (¼-wave stub opposite the cavity, vacuum pump port directly under the tee, RF window assembly connection, and the cavity connection that tapers to ϕ100-mm through a distance of 207-mm at the thermal intercept). The matching collar of the IC and ¼-wave stub match the RF impedance. A fixed-tip IC and an adjustable-tip IC design were tested. The adjustable-tip design is shown in Figure 3. Additional information about the mechanical and RF design is contained in another reference [2].

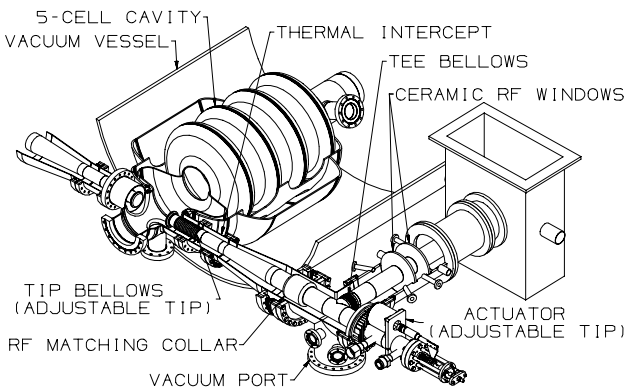

Figure 1: Power coupler and RF window assembly

2.2 Analysis & Verification

The thermal design of the power coupler is addressed in other references [2][3]. To verify the cryogenic heat leaks and other thermal calculations, the cryogenic test rig (CTR) was built. This was a dewar that suspended the power coupler in 4 K liquid He that had simulated RF losses. It included the use of the thermal intercept. The results were found to be in good agreement with the thermal model. However, certain enhancements had to be made to the model. The thermal interface impedance at each Conflat vacuum flange on the OC was found to be important in matching the predicted and measured

* Supported by the US Department of Energy, Defense Programs
† schmierer@lanl.gov

temperature distributions. This added two thermal resistances to the model. The measured heat leak is largely dependent on the low temperature intercept temperature, which in a cryomodule will vary from one coupler to the next because they are in series.

The antenna tip movement of the IC relative to the cavity was analyzed. Thermal contraction of the OC and expansion of the IC results in a relative change of 0.035-in. between the IC tip and the OC junction with the cavity, resulting in tip insertion. This changes Q_{ext} by a factor of 1.08. This Q_{ext} effect should be considered if implementing the fixed-tip power coupler design. Lateral antenna tip movement from dynamic motion was calculated applying the Ground Test Accelerator Design Envelope power spectral density [4] as a random vibration to the IC. The absolute displacement towards the cavity is 0.0038-in., which is approximately half of what was considered the maximum allowable lateral offset due to dynamic motion (0.5% change in Q_{ext}). Displacement induced from the vacuum pump was negligible except during startup and shutdown of the turbo pump. The tip penetration into the beam tube is 3.2 times more sensitive than lateral displacement.

2.3 Fabrication

The quantity of coupler/windows required for the APT linac is 242, with one for each SC cavity. Separate vendors fabricated the individual prototype components.

The RF window assembly was designed and fabricated by CPI, Inc. (Palo Alto, CA) and Marconi Applied Technologies (Chelmsford, England, UK formerly EEV, Ltd). These vendors were responsible for all analysis, bench-top testing, and fabrication. The ceramic is AL995. The airside T-Bar and its inner conductor are air-cooled, as is the region between the two ceramics. The units underwent low power testing at the vendor facility and were high power acceptance tested at LANL. Only the RF window assemblies manufactured by Marconi were used for room temperature testing with the power coupler. A total of ten RF window assemblies were fabricated.

Ten outer conductors, eight inner conductors, and seven thermal intercepts were fabricated. The major issue with inner conductor fabrication was procurement of bellows in the small quantities of custom geometry required. Attaching bellows to the structure was also difficult, electron-beam welding was the method finally adopted.

A manufacturing study was performed on the prototype coupler/window assembly design that gave us information about the cost of plant-scale quantities and the facilities required to do such work [5].

3 HIGH POWER TESTING

3.1 Test Stand & Procedures

Power coupler/window assemblies were tested on the Room Temperature Test Bed (RTTB) [6]. Up to 1 MW, CW RF power was available from a 700-MHz klystron. Two power coupler/window assembly pairs were coupled by a copper pillbox cavity in the TM_{010} mode.

Before testing, the inner conductors and outer conductors received either a Citronox degreasing or were just wiped with a lint-free cloth and methanol. The RF window assemblies were installed on the test stand directly from their crates. They were removed once from the RTTB during testing to be grit-blasted.

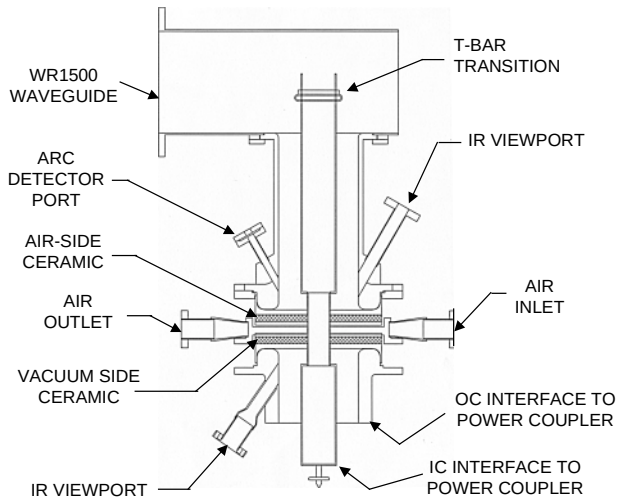

Figure 2: Schematic of the RF window assembly tested with the power coupler on the room temperature test bed

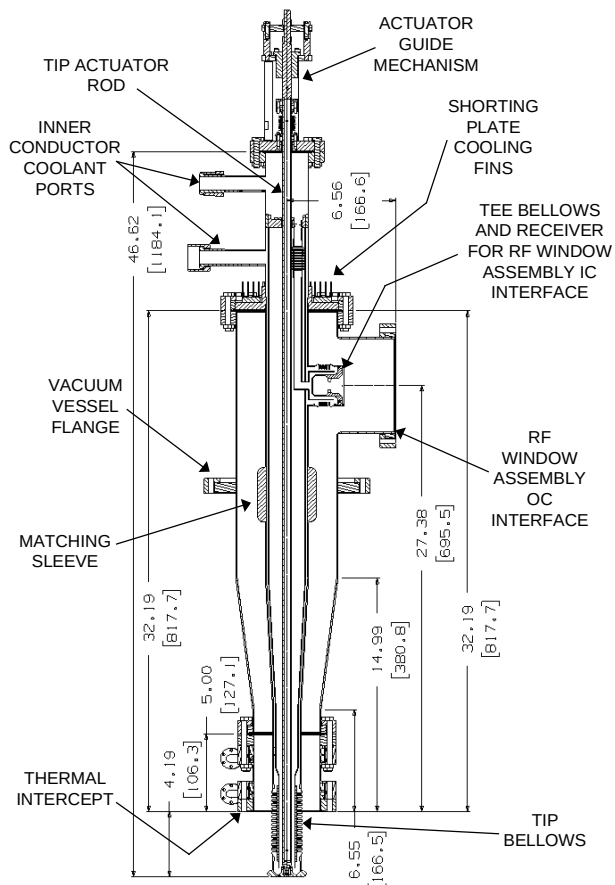

Figure 3: Power coupler schematic (adjustable-tip design)

Prior to high power testing, all the sets of components were tested at low power using a HP 8753E network analyzer. Measurements were taken from the waveguide of the input RF window assembly to the output RF window assembly waveguide using WR1500 waveguide to BNC adapters. With this setup, the maximum VSWR measured for all combinations of components was less than the required 1.04. Figure 4 is a typical transmission plot for a set of components.

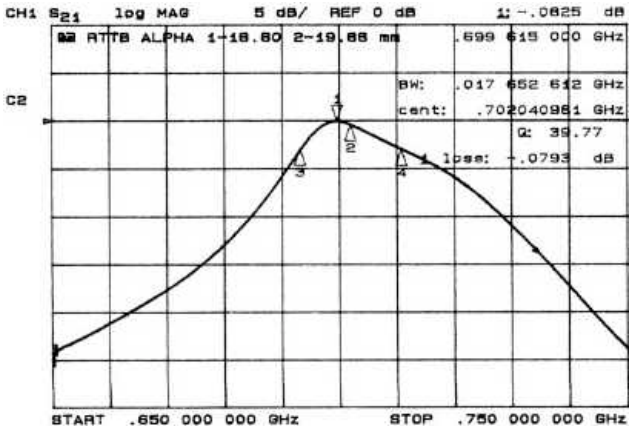

Figure 4: Typical transmission of a set of components encompassing an assembly pair and cavity on the RTTB

3.2 High-Power Tests and Results

Four general tests were performed: (1) transmitted-power, (2) totally reflected power, (3) condensed-gas effects, and (4) longer-term steady power transmission.

During transmitted-power capability tests, RF power was transmitted from the klystron, through the couplers, and into the RF load. This included the conditioning phase, where the power level was continually raised in steps to reach the desired power level. During this, the pressure was kept below 5 x 10^{-6} torr. Results from the first fixed-tip power couplers tested are in reference [7], and results from the adjustable-tip coupler transmission testing in [8]. Both designs reached 1 MW, CW, with the klystron dictating maximum power levels.

There appeared to be a correlation between the residual gas magnitudes and conditioning time rather than conditioning rate. The conditioning rate is the transmission power level increase per unit time of conditioning. The conditioning time when H_2 became the dominant residual gas was consistent, about 12 hours for conditioning rates of ~23 kW/hr and ~31 kW/hr.

For reflected-power testing, a "sliding short" allowed movement of the standing-wave maxima and minima in λ/16 increments. The tests reached 850 kW, CW for a sliding-short position corresponding to full current, "open cavity" situation. For all other short positions, we reached a power level of 550 kW, CW and a power level of 850 kW at a duty cycle of 50%. Limits were due to maximum temperature constraints on the RF window housing [7].

To investigate the condensed-gas effects, we cooled the outer conductor by passing liquid nitrogen through the channels of the thermal intercept [8]. Based on the partial pressures of the residual gases, water vapor and CO_2 were expected to condense on the inner surface of the OC during these tests. A surface temperature of ~30 K would be required to condense other gases. Therefore, it was deemed that testing with a colder outer conductor wouldn't add significant information about the coupler performance. This method was sufficient for determining multipacting effects in the CERN LEP2 power coupler [9]. Temperature distribution of the OC for different power levels is shown in Figure 5.

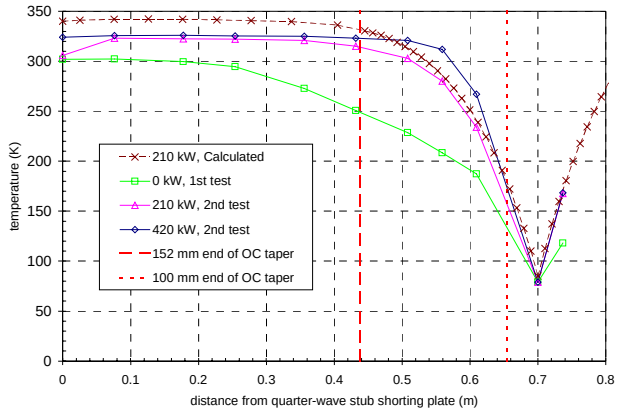

Figure 5: Temperature distribution of OC versus power level with LN_2 circulating through thermal intercept

Figure 6 shows an example of data obtained. For this data, erratic vacuum behavior begins at 9:45 before the components are cooled and increases after the cooling begins at 10:30. In general, the erratic vacuum behavior wasn't necessarily consistent with temperature or power level.

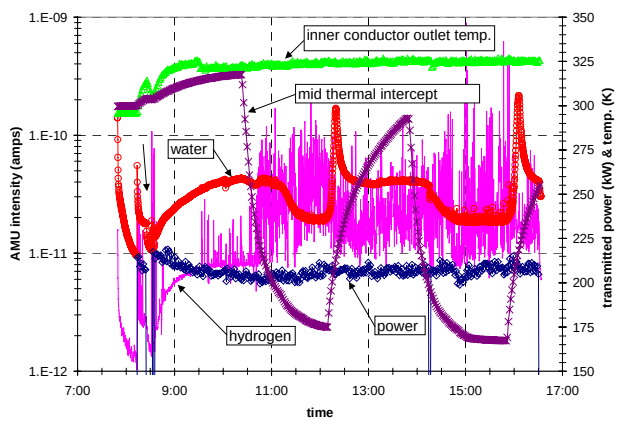

Figure 6: Residual gas intensity (hydrogen & water left axis) with transmitted power, mid thermal intercept temperature, and inner conductor outlet coolant temperature (power & temperatures right axis) after 34 hours of testing at 210 kW

A final condensed-gas experiment consisted of putting a large amount of air into the vacuum space and then trying to recover from that. This was performed with adjustable tip couplers with the outer conductor at liquid nitrogen temperatures on two occasions. The first time, 2018

standard cm^3 of air was added to the vacuum space. The vacuum system shutdown the RF due to the high pressure, it then took the next three hours to condition back to 420 kW. During this time there were multiple shutdowns of the klystron due to arcs and over pressures. The arcs and pressure bursts are from the reconditioning of the surface as condensed gases are removed.

Longer term testing was performed at 420 kW, which had recently become the baseline design power requirement. During this testing, a certain power level was obtained and then maintained for a given amount of testing time. The longest run was 95 hours at 420 kW. During initial conditioning the pressure range is 1×10^{-7} – 5×10^{-6} torr. With RF on after conditioning it resides in the 1×10^{-8} – 1×10^{-7} torr range. The pressure is typically a factor of five less with the RF off. During steady-state testing the vast majority of the interruptions in power were klystron false positive trips and not arcing.

4 OBSERVATIONS DURING TESTING

4.1 Tip Bellows Failure

During testing of adjustable-tip IC's on the RTTB, two failures of tip bellows occurred. Material analysis performed on the failed bellows determined the bellows material, Be-Cu, over-aged. This reduced the ultimate strength below the high stresses caused by the thermally induced displacements, allowing failure along the grain boundaries. The high temperatures (~400°C) that the inner conductor bellows experienced were due to cooling with air instead of He and testing at power levels significantly higher than the 500 kW, CW thermal/mechanical design. Reengineering of the tip region and/or using He coolant would be required for sustained operation of the adjustable-tip inner conductor over 500 kW, CW.

4.2 Arcing

During conditioning, arcing occurred on the vacuum side of the windows primarily. After a power level had been conditioned to, no more arcs were seen below this power level. Arc rates varied between component sets but generally increased in the 200 – 350 kW power range. This corresponds to the regions of heightened vacuum activity observed during the testing (see section 4.6). Anomalous arcing occurred in two instances due to a poor connection of the receiver cup to the inner conductor of the RF window assembly. This was corrected by reassembling the components.

4.3 Electron Etching

All inner conductors tested had evidence of electron activity on their surface (see Fig. 7). The outer conductors had no signs of this. These patterns varied in concentration and position with each test as well as with power level. At power levels between 210 and 500 kW, they were typically only shallow, dendrical patterns. Above 500 kW, the patterns were deeper and more concentrated in a single spot. The occurrences of the electronic etching didn't correspond to arc measurements, nor did it affect coupler operation. It is believed that this was due to the surface condition. A foreign material may have been introduced during final polishing of the surface at the vendor or it may just be particulate from installing in open areas with no air filtration. The etching didn't occur on an electroplated inner conductor tested at 420 kW, which supports the foreign material theory. There is also some evidence that it occurs only during conditioning and is not a continual process.

Figure 7: Electronic etching on inner conductor

4.4 Coaxial Conductor RF/Vacuum Seals

The vacuum seals of the outer conductor that carried RF current performed well. We used standard high-vacuum flange connections with the inner edge radiused to 0.040". We also used a modified copper gasket. The inner diameter of a standard Cu gasket was enlarged so the edge recessed by 0.040" and had a 0.040" radius on the inside. We experienced no difficulties with this design as far as RF power transmission, and there was no visible damage after testing to > 1 MW. The stainless steel flange was electro-plated up to the base of the knife-edge. In one case where the plating had gone up the side of the knife-edge, the gasket wouldn't seal properly. Figure 8 shows the geometry of this joint.

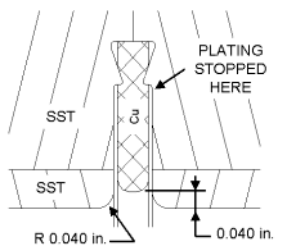

Figure 8: Cross-section of the outer conductor RF joint with modified vacuum flanges and gasket

4.5 RF Window Assemblies

The total hours of operation of the window assemblies above 210 kW were estimated at 650 window-hours. No problems were encountered with RF transmission or

cooling of the window assemblies at or below 420 kW. At power levels over ~450 kW the output vacuum side window would glow orange around the braze joint of the inner conductor. This ceased after grit-blasting the window. At power levels of ~850 kW and above, the vacuum side windows glowed blue over the surface. This was not reconfirmed following grit-blasting. The requirement to rotate the RF window assembly during installation led to damaging two of three units tested and damage to one inner conductor. This feature would be reconsidered in future designs.

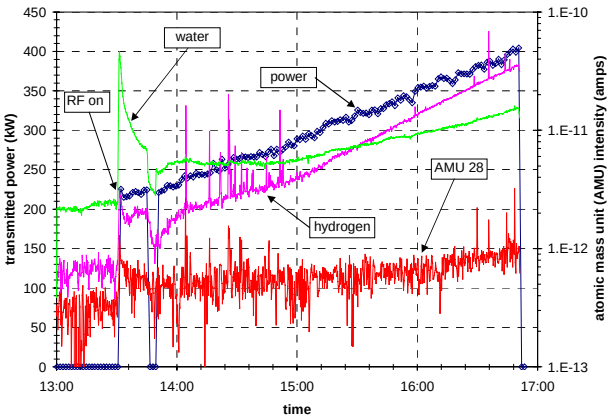

Figure 9: Residual gas magnitude (right axis) and power level (left axis) versus time during a room temperature power level sweep to look for multipacting power levels

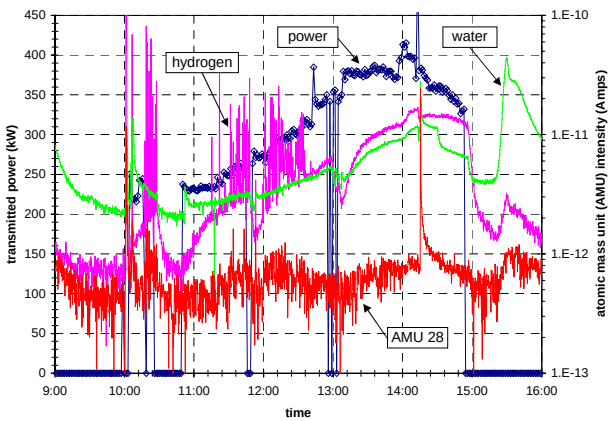

Figure 10: Intensity of residual gases and power level versus time with liquid nitrogen circulating through thermal intercept

4.6 Multipacting

There were no hard multipacting barriers encountered during conditioning to 1 MW, which typically took 24 hrs. There were some indications of soft bands from erratic vacuum activity in the 250-350 kW range. To quantify this, the power level was slowly swept up and down between 200 and 400 kW at room temperature and with LN_2 in the thermal intercept. One example of this for room temperature is shown in Figure 9 and with the OC cold in Figure 10. No specific power level could be discerned, and testing cold only enhanced the same effects. We believe the lack of major multipacting affects is due to the excellent vacuum pumping near the window. Coaxial dimensions and frequency also place the design in a regime where we were perhaps only encountering the 5th and higher modes of single point multipacting.

5 DEVELOPMENT SUMMARY

- APT power coupler and RF window assembly development occurred from 1997 to 2000.
- The ability to fabricate the prototype coupler/window assembly in small quantities was demonstrated with no major difficulties.
- Performance in terms of RF power capability was demonstrated by tests of both fixed and adjustable coupling power couplers up to 1 MW, CW traveling-wave and 850 kW, CW standing-wave power.
- Only minor indications of multipacting were seen during conditioning. Testing with the taper end of the outer conductor at liquid nitrogen temperatures only enhanced the vacuum activity in the power levels of 250 – 350 kW. Recovery from a vacuum failure with the outer conductor cold took approximately 3 hrs.
- Minimal multipacting issues are attributed to the coax sizing, frequency, and excellent pumping near the window.

6 REFERENCES

[1] G. P. Lawrence, "High-Power Proton Linac for APT; Status Of Design And Development," LINAC98 Proceedings (1998).

[2] E. N. Schmierer, et. al., "Development of the SCRF Power Coupler for the APT Accelerator," PAC99 Proceedings (1999).

[3] J. A. Waynert & F. C. Prenger, "A Thermal Analysis and Optimization of the APT 210 kW Power Coupler," LINAC 98 Proceedings (1998).

[4] W. O. Miller, "GTA Facility Vibration Spectrum – PSD Format," LANL memorandum MEE-12-372-89, August 1989.

[5] LANL Report: LA-UR-01-0030, "APT ED&D Coupler/Window Manufacturability Assessment: Final Report," December 2000.

[6] J. Gioia, et al., "A Room Temperature Test Bed for Evaluating 700-MHz RF Windows and Power Couplers for the Superconducting Cavities of the APT Linac," PAC99 Proceedings (1999).

[7] E. N. Schmierer, et al., "Testing Status of the Superconducting RF Power Coupler for the APT Accelerator", 9th RF Superconductivity Workshop Proceedings (1999).

[8] E. N. Schmierer, et al., "High-Power Testing of the APT Power Coupler", LINAC 2000 Proceedings (2000).

[9] Haebel, E., et. al., "Gas condensation on cold surfaces, a source of multipacting discharges in the LEP2 power coupler," 7th RF Superconductivity Workshop Proceedings (1995).